

pubs.acs.org/JPCA Article

Reaction Pathway Analysis of PET Deconstruction via Methanolysis and Tertiary Amine Catalysts

Rishabh Sanghavi, Nadia N. Intan, Shaoqu Xie, Hongfei Lin, and Jim Pfaendtner*



Cite This: J. Phys. Chem. A 2024, 128, 5883-5891



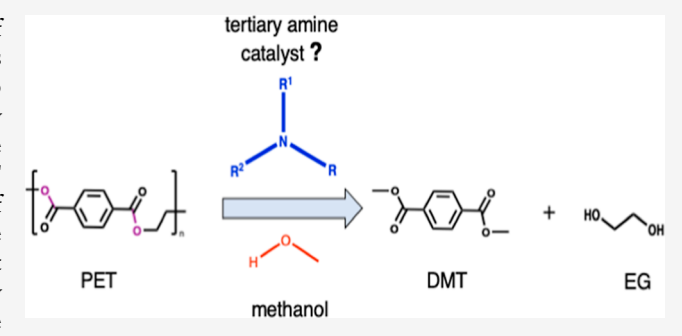
ACCESS I

III Metrics & More

Article Recommendations

s Supporting Information

ABSTRACT: Polyethylene terephthalate (PET) is a type of polymer frequently used in plastic packaging that significantly adds the amount of plastic waste found in landfills. One of the ways to recover valuable raw materials from postconsumer plastic is by depolymerizing PET into its monomeric constituents, which are dimethyl terephthalate (DMT) and ethylene glycol. PET depolymerization is often done in methanolysis with the help of acidic or base catalysts. Tertiary amine is one of the most attractive base catalysts for PET depolymerization in methanolysis since it does not lead to the generation of potentially environmentally harmful waste, unlike metal-based catalysts. However, the mechanism by which tertiary amines catalyze PET depolymeriza-



tion in methanolysis remains unexplored. Developing a detailed mechanistic understanding of this process is important for improving plastic upcycling since it opens the possibility of employing various cheaper and more environmentally friendly reaction conditions. Using density functional theory and transition state analysis, we show that in the presence of tertiary amine catalysts, methanolysis of PET consists of multiple discrete-step reactions rather than a single concerted step. Furthermore, by comparing our calculations to recent experimental results, we were able to rationalize the DMT yield from the depolymerization process by relating it to charge polarization within tertiary amine catalysts, thus opening a pathway to identify atomic descriptors for future catalyst design.

INTRODUCTION

Plastic is made of synthetic polymeric materials with a wide range of applications in our everyday life from textiles to packaging. Since the 1950s, there have been more than 10 billion t of plastic produced, with more than 80% found to have ended up in landfills as waste. With only less than 10% of the postconsumer waste having been recycled, accumulation of plastic waste is a pollutant that has become harmful to both animals and humans. 4

Thermoplastic resin polyethylene terephthalate (PET) used primarily in packaging containers, cups, or bottles accounts for 10% of the global plastic resin production. PET also has a high recycling rate of 20% in the US making it an important polyester of interest for polymer upcycling. PET can be recycled through several methods, including reactive extrusion, mechanical recycling, energy recovery via incineration, or chemical recycling through depolymerization to its constituent monomers. One approach within chemical recycling that has gained significant traction for PET depolymerization is solvolysis, which includes methods such as hydrolysis, methanolysis, 11–13 glycolysis, 14–16 ammonolysis, aminolysis, or in the presence of enzymes. Based on reaction conditions such as heat, catalyst, and solvolysis method, PET breaks to form either terephthalic acid, dimethyl terephthalate

(DMT), or bis(hydroxyethyl) terephthalate (BHET) monomer. ^{12,15,20,21}

Methanolysis of PET is a transesterification reaction that depolymerized PET into ethylene glycol (EG) and DMT monomer, which are produced in accordance with reaction Schematic 1.

Both EG and DMT monomers in Schematic 1 can be recycled back to reform polymer of similar quality as PET. ²² Unfortunately, the alcoholysis of PET is a kinetically slow reaction without a catalyst. Much lower yield of DMT and EG are reported for the methanolysis of PET in the absence of a catalyst. ¹³ It is reported that at 200 °C in the absence of a catalyst, methanolysis of PET in 100 mL of methanol results in 2.9 and 3.6% yield of DMT and EG, respectively. Under the same conditions but with the addition of 50 mg of aluminum triisopropoxide as catalyst, the yields of DMT and EG increase to 67.3 and 68.3%, respectively. ¹³

Received: April 7, 2024 Revised: June 10, 2024 Accepted: June 18, 2024 Published: July 11, 2024





Scheme 1. Depolymerization of PET via Methanolysis to Form DMT and EG

The introduction of base catalysts results in the increase of the electrophilicity of the ester group, which results in the ester becoming more prone to nucleophilic attack by the oxygen in the methanol solvent (the ester bond is drawn in purple in Scheme 1). The reaction between the ester group of PET and the methanol solvent results in the creation of a tetrahedral intermediate, which facilitates proton transfers from methanol to ester. The ester and methanol reaction generates a water molecule in addition to a resultant ester that will rearrange to form ester product and regenerate the catalyst. ²³

Several experimental studies have extensively studied PET methanolysis using basic catalysts such as potassium carbonate, 12 zinc acetate, magnesium acetate, or cobalt acetate. 24-27 However, reports on the effectiveness of methanolysis as a means to depolymerize PET are varied and are dependent on experimental conditions, some of which include type of metal-based catalyst, molecular weight of PET and use of vapor or supercritical methanol for methanolysis. In lieu of using metal-based catalysts during the methanolysis process to depolymerize PET, a more environmentally friendly alternative is organic amine-based catalysts. Amines, which are Lewis bases, are known to accelerate the transesterification reactions as catalysts. 28 These hydrogen atoms in both primary and secondary amines may react with the carbonyl group of PET, which results in an amidation process that leads to the formation of amide. The resulting amides are not as strong Lewis bases compared with the original amines.

In contrast, tertiary amines have no hydrogen atoms attached to nitrogen and thus do not readily lead to amidation reactions to form a less basic amide. However, the basicity of tertiary amine catalysts is significantly affected by steric hindrance of nitrogen, which can have an opposing effect on catalyst reactivity.²⁹ Hence, there are competing factors that make tertiary amines beneficial and detrimental as catalysts for PET depolymerization. However, the exact mechanism in which the tertiary amine catalyzes PET depolymerization is yet to be understood, much less the knowledge on how to choose the suitable tertiary amine molecules to help catalyze the PET depolymerization reaction. In this study, our goal is to attain a comprehensive understanding of how a tertiary amine catalyzes PET depolymerization and unveil the important factors of the tertiary amines that determine their efficiency. We use density functional theory (DFT)-based methods to study the depolymerization mechanism in the presence of various tertiary amine catalysts. In this study, we select six tertiary amines with recently published experimental data for this reaction.³⁰ We studied PET depolymerization via methanolysis to determine its reaction mechanism. We also explore the effect of methanol solvent and tertiary amine catalysts on the reaction energetics. We then compare our calculated results to that of the experimental yield in which we unveil the correlation between the experimental yield and the charge on the N atom of the protonated tertiary amine catalysts. Finally, we propose a descriptor in which prediction of the efficiency of

potential catalysts can be used to accelerate the discovery of future catalysts.

The rest of the paper is organized as follows: first, we describe the computational procedure used in this study. Following this, we present our results, in which we investigate the PET depolymerization reaction mechanism. We systematically increased the complexity of our system to understand the effect brought by methanol solvent and tertiary amine catalysts on the energetics of the PET depolymerization reaction. We finally compare our computational results to previously published experiments to gain insights into factors that affect the yield in PET depolymerization. In the end, we provide a quick discussion in which we propose a descriptor that can be employed to quickly predict the effectiveness of other tertiary amines as potential catalysts for PET depolymerization.

METHODS

DFT calculations were carried out using the Gaussian16 software package.³¹ Geometry optimizations were performed using the Minnesota M06–2x³² hybrid exchange–correlation functional together with the 6-31G (d,p)^{33,34} basis set for all atoms. The M06-2x hybrid exchange-correlation functional was used because of its wide applications in the main group for thermochemistry and kinetics. 32 The effect of methanol solvent on the depolymerization reaction was studied through the incorporation of the polarizable continuum model using the self-consistent reaction field method keyword. 35-39 Prior to precise determination of transition states, reaction mechanisms was explored with constrained geometry optimizations 40 and eventually saddle points on the potential energy surface were determined with full transition state optimization (keyword = TS). Transition states were verified by confirming that there was only one imaginary frequency for the resulting vibrational frequencies calculated (keyword = freq). They were further verified by following the reaction path by performing intrinsic reaction coordinate (IRC)⁴¹ (keyword = IRC) calculations followed by geometry optimization after the IRC calculation is complete. We provide example input files for transition state, IRC scan, and geometry optimization calculations in Supporting Information A1.

We describe the methanolysis reaction primarily with a simplified set of descriptors (bond distances) that undergo significant change. As shown in Figure 1, R1 defines the distance between ester carbonyl carbon and methanol oxygen, while R2 denotes the distance between ester oxygen and methanol hydrogen. Later in the study, we added tertiary amine catalyst, which were placed adjacent to the transition state, but not obstructing the reaction pathway. The atomic charges and proton transfer energy were calculated using the CHELPG method⁴² at the M06–2x³² functional and the 6-311++g (d,p) 43,44 basis set. GaussView and PLUMED version 2.8^{45,46} were used for bond analysis. We note that 6-311++g (d,p) has been used previously to calculate atomic charges



Figure 1. Key atomic distances used to describe ester methanolysis reactions in this study.

using the CHELPG method^{47,48} and is used additionally for geometry optimization calculations.⁴⁹

RESULTS

Methyl Ester Base Case: Obtaining Transition State Structure. The methanolysis reaction is complex, requiring multiple concerted bond breaking and forming events. We initially performed a detailed characterization of the methanolysis of methyl ester with the goal of characterizing the

simplest methanolysis reaction possible and learning if the model transition state from that reaction could be applied to the study of PET methanolysis. Using constrained geometry optimization, we studied three different approaches of the methanol molecule to the ester linkage, by varying the corresponding distances R1 and R2 in a stepwise fashion $(\Delta R = 0.1 \text{ Å})$, as shown in Figure 2.

We first study the scenario in which the methanol oxygen attacks the carbonyl linkage at the carbon atom (R1) (Figure 2a). Note that here, the distance between the methanol hydrogen and ester oxygen is monitored but not controlled (R2 is shown on the secondary y-axis in Figure 2a). Decreasing the distance progressively increases the potential energy until the energy goes through a maximum around R1 = 1.2 Å, at which point R2 also drops precipitously. Using the structure with an energy maximum as an initial guess, we performed multiple rounds of attempt/refinement to identify a TS structure with different algorithms for determining saddle points. None of the attempts were successful. We next attempted the same study but constraining and varying R2

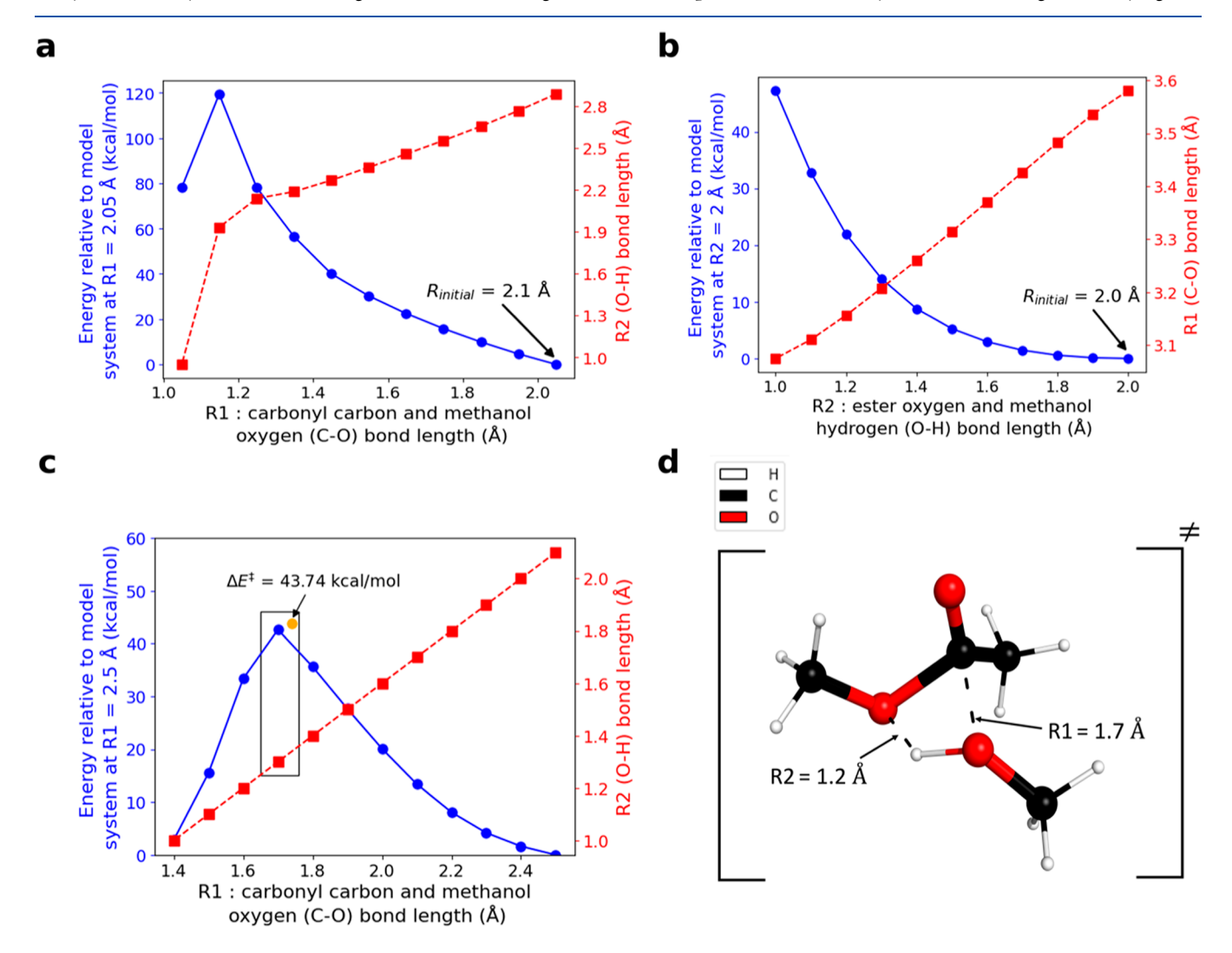


Figure 2. Changes in energy and bond length as the result of stepwise scan of (a) C-O distance between carbonyl carbon and methanol oxygen (R1), (b) O-H distance between ester oxygen and methanol hydrogen (R2), and (c) R1 and R2 together, where the distances of both R1 and R2 were simultaneously reduced by 0.1 Å. The black box signifies the maximum energy that was achieved when the C-O R1 distance = 1.7 Å and O-H R2 distance = 1.3 Å, respectively. The structure of this maximum energy was used as the initial guess for transition state finding. The transition state structure is shown in (d).

while monitoring R1 (Figure 2b). Here, the system never passes through any maximum of energy and there are no apparent reactions occurring. Monitoring the resulting structures clearly indicates the methanol is not oriented in a fashion that can facilitate the required concerted bond breaking and formation events. Hence, R1 and R2 alone are not suitable proxies for the reaction coordinate and therefore cannot be scanned independently to determine an initial guess for transition state finding calculations.

Next, we simultaneously scan both R1 and R2 together using multiple constraints in the geometry optimization. We established initial distances of R1 and R2 to 2.5 and 2.1 Å, respectively; we then simultaneously reduce the distances of both R1 and R2 by steps of 0.1 Å. The relative energy from this simultaneous scan of R1 and R2 is shown in Figure 2c. As shown, the relative energy peak 42.6 kcal/mol is observed when R1 and R2 are of 1.7 and 1.3 Å, respectively. This configuration is used to search for a transition state and the resulting calculation shows a structure with very similar energy and one imaginary vibrational mode $(-1179.9 \text{ cm}^{-1})$. The TS structure (Figure 2d) is extremely similar in geometry (R2 is only adjusted by 0.1 Å) and energy (the TS structure is 1.1 kcal/mol higher at 43.7 kcal/mol). We also confirm the configuration at the transition state by doing an IRC scans from the transition state to both the reactant and product states.

For the remainder of this study, we use the transition state configuration shown in Figure 2d as the starting point for other systems involving more complex models, such as when we replace the methyl ester with a more realistic representation of PET. In the following sections, we study different surrogates of PET decomposition with a longer alkyl chain length attached like ethyl benzoate and then introduce a set of tertiary amine catalysts explicitly into the system to study the effect of catalysts on PET depolymerization. Finally, the solvent effect on depolymerization reaction energetics would also be discussed.

Increasing Surrogate Complexity. We now replace the methyl ester with a more realistic representative of PET, ethyl benzoate. To determine the ethyl benzoate methanolysis reaction mechanism, we began by using the transition state structure described above, we replaced the methyl group connected to the C=O linkage with a benzyl ring. We froze the coordinates of all four atoms involved in the concerted bond breaking and forming and performed geometry optimization and frequency calculation. The structure showed one imaginary vibrational mode of similar frequency to the TS described above (as shown in Supporting Information Table A2). Following this, we determined a saddle point TS structure and used the IRC scan as a means to obtain a detailed mechanistic understanding of the methanolysis process while verifying that the obtained TS structure leads to the correct reactants and products.

The reaction between ethyl benzoate and methanol is shown in Figure 3a, whose progress we track by monitoring the R1 and R2 bonds. The R1 and R2 bonds are defined in Figure 1. Furthermore, we also track the evolution of the improper dihedral formation by the four key atoms defined by R1 and R2, as shown in Figure 3a. The improper dihedral is thus defined as the angle between the i, j, k, and l planes, where i, j, k, and l refer to methanol hydrogen, ester oxygen, carbonyl carbon, and methanol oxygen, respectively.

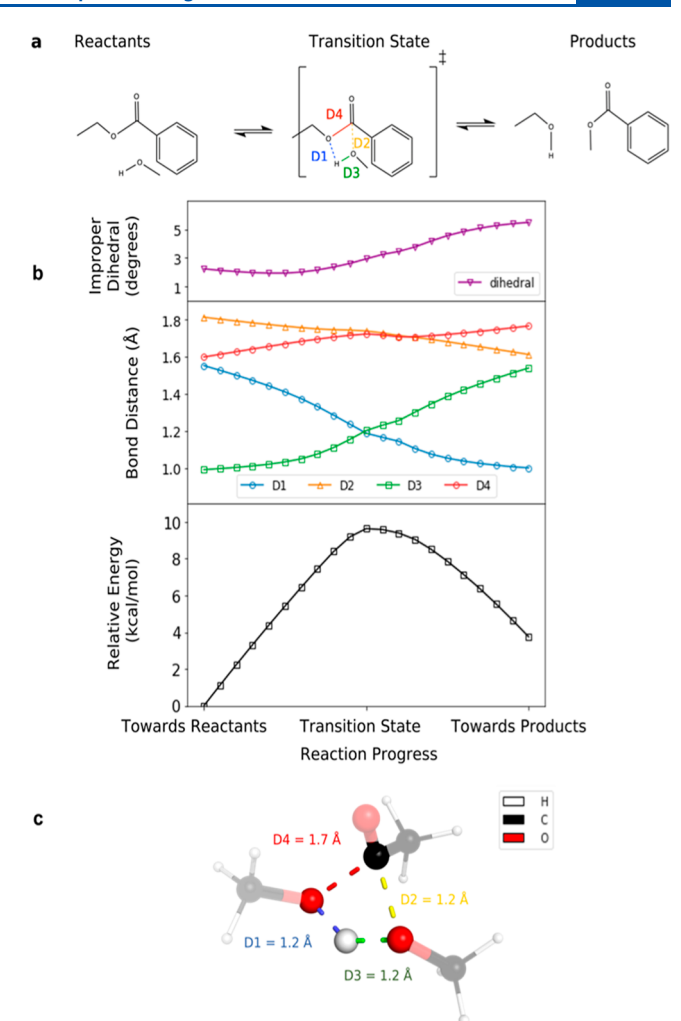


Figure 3. (a) Overall reaction schematic for ethyl benzoate during methanolysis of ester. The reaction progress is tracked through the evolution of bonds D1–D4. (b) The corresponding bond distances (Å), improper dihedral (degrees), and relative energy (kcal/mol) of reaction with respect to 11th IRC step going toward reactants. (c) The tetrahedral complex model showing bonds D1–D4.

From Figure 3b, we can deduce the order of events in the methanolysis reaction mechanism between ethyl benzoate and methanol to be as follows:

- The reaction begins as hydrogen of methanol breaks away from methanol oxygen toward ester oxygen leading to decrease in bond distance D1 (blue),
- Simultaneously, the distance between methanol oxygen and methanol hydrogen increases as shown by D3 (green), until D1 and D3 curves intersect at the transition state.
- 3. After reaching the transition state, the hydrogen continues to move toward ester oxygen and breaks away from methanol, as shown by further decrease in the D1 distance. This corresponds to a decrease in the relative energy.
- 4. The carbonyl carbon and methanol oxygen then move closer toward each other as shown by the decrease in the D2 (yellow) distance.
- 5. The C-O ester bond in ethyl benzoate breaks as the carbonyl carbon and ester oxygen move away from each other, shown by the increase in D4 (red). Finally,

The carbonyl carbon then forms a bond with methanol oxygen to form products methyl benzoate and ethanol.

Figure 3b also shows that improper dihedral changes very slightly from ~ 2 to $\sim 6^{\circ}$ moving from the reactant to the product complex. This change is relatively small, indicating that the improper dihedral is relatively unchanged in planar configuration of the four atoms described in step 3 above. The transition state for the methanolysis reaction between ethyl benzoate and a methanol is formed in a concerted fashion as all four key bonds in the tetrahedral intermediate (D1–D4) are broken and formed in the same step, as shown in Figure 3c.

In Figure 3b, we note that the labels "Toward Reactants" and "Toward Products" refer to the relative energy of the 11th IRC step in the direction of reactants and products, respectively. In Gaussian 16, IRC by default takes 10 steps from the transition state. Including the transition state, the "Toward Reactants" and "Toward Products" are the 11th IRC step in their respective directions. Each step is represented by a square marker in the relative energy plot in Figure 3b.

Effect of Tertiary Amine Catalysts on the PET **Methanolysis.** In this section, we explore the role of tertiary amine catalysts in the transesterification reaction of ethyl benzoate and methanol. The work described above indicates that proton transfers from methanol directly to ethyl benzoate oxygen to break the ester bond as detailed in Figure 3. Transesterification occurs through a single concerted step. In the model system, the catalyst is on the opposite side of the aromatic ring of ethyl benzoate away from methanol, such that it does not directly participate in the proton transfer step of the reaction. It has been proposed that tertiary amine catalysts act as Lewis base in methanol due to free electrons of N atom and could possibly form a hydrogen bond between N of catalyst and H of aromatic ring in ethyl benzoate and another hydrogen bond between H atom on methyl adjacent to N atom and carbonyl carbon to activate the ester bond.³⁰ Therefore, the role of this catalyst in lowering the activation energy could primarily be expected to result from the activation of ester from these hydrogen bonds.

To understand this effect we introduce a list of tertiary amine catalysts whose effectiveness in depolymerizing PET have been investigated experimentally.³⁰ The list includes linear, cyclic, aromatic, and diamines, whose chemical structures are given in Figure 4. Reported experimental yields of DMT, EG, and total yield are shown in Table 1 for the list

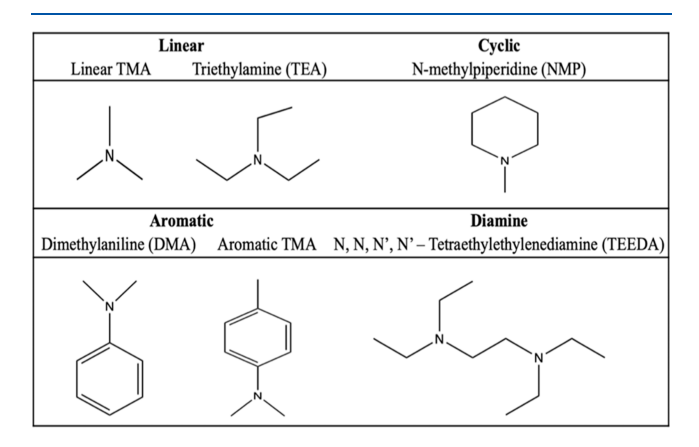


Figure 4. Six different tertiary amines used in this study as representatives to understand the effect of amine catalysts on the PET depolymerization reaction by methanolysis at the atomistic level.

of catalysts. Table 1 does not include values for linear TMA as it is not part of the experimental study.³⁰

Table 1. Yields of DMT, EG, and Total Yield from Depolymerization of 0.1 g PET Bottle Strips in 20 mL of 0.20 M Tertiary Amine Methanol Solution at 160 $^{\circ}$ C, 1 h Reaction Duration at 700 rpm 30a

		yields (%)		
catalysts	catalyst configuration	DMT	EG	DMT + EG
NMP	cyclic	100	100	200
TEA	linear	91.2	74.5	165.7
aromatic TMA	aromatic	25.8	14.3	40.1
DMA	aromatic	6.4	6.8	13.2
TEEDA	diamine	80.1	85.1	165.2

"Yield is calculated from moles of DMT and EG after the reaction in accordance with the formula shown in Supporting Information A3.

Using ethyl benzoate as the representative model for PET, the overall energy landscape of the PET depolymerization through methanolysis in the presence of tertiary amine catalysts are shown in Figure 5.

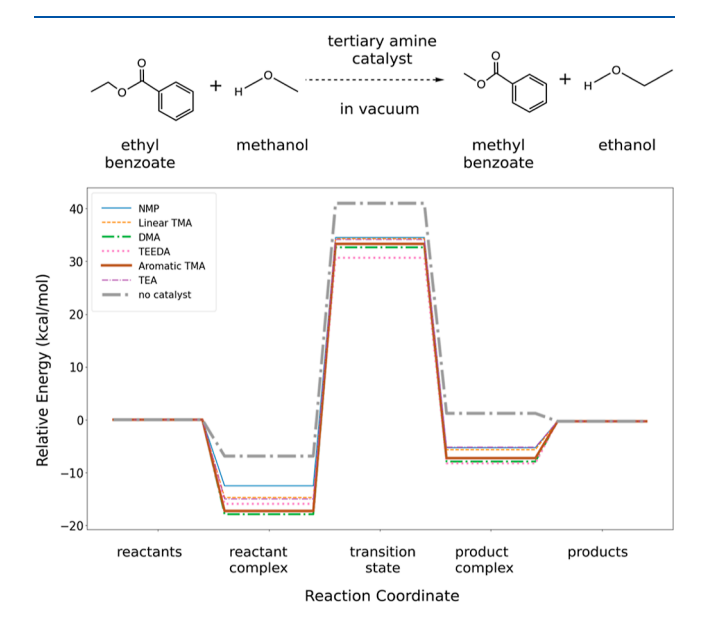


Figure 5. Effect of tertiary amine on the energy landscape of transesterification reaction between ethylbenzoate and methanol in a vacuum. The energies for reactant, transition, and product states were calculated through geometry optimizations. Energies for the reactant complex and product complex were obtained through geometry optimization of the final IRC structures in each respective direction and the reactant/product energies are the summation of the individual species energies.

Figure 5 clearly shows that the presence of tertiary amine successfully lowered the activation barrier for the transesterification of ethyl benzoate by methanol, thus showing its promising potential to catalyze PET depolymerization in methanolysis. Furthermore, the effectiveness of the tertiary amine in lowering the activation barrier in the ascending order from the lowest activation barrier is TEEDA, DMA, aromatic TMA, TEA, linear TMA, and NMP, respectively. The ordering of the tertiary amine in catalyzing the reaction in Figure 5 can be clearly classified based on the structures of the tertiary amines as defined in Figure 4, where the lowest transition state

is obtained by the diamine type of tertiary amines, that is followed by aromatic, linear, and cyclic types, respectively.

However, we stress that the energies for the transesterification reaction of ethylbenzoate shown in Figure 5 were obtained from calculations in a vacuum. PET methanolysis in experiments however occurs in methanol solvent. Product yield results in Table 1 were reported for the reaction using a tertiary amine methanol solution. Hence, we introduce methanol solvent into our study to study the effect of solvation to the PET depolymerization through methanolysis.

Effect of Solvation. To study the effect of methanol on the PET depolymerization reaction during methanolysis, a methanol solvent is introduced into the system implicitly. Methanol molecule and ethyl benzoate are present in the system as reactants along with the tertiary amine catalyst. The energy landscape of the ethyl benzoate transesterification reaction in the presence of tertiary amines in implicitly treated methanol is shown in Figure 6.

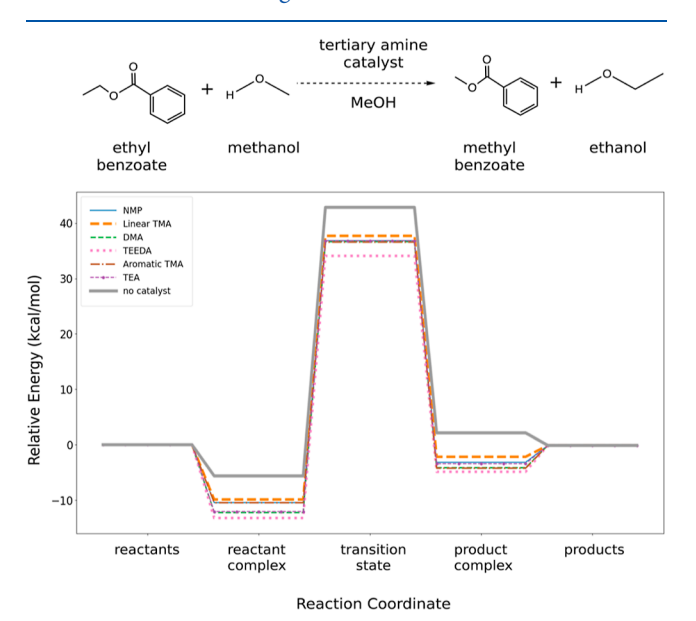


Figure 6. Effect of tertiary amine on the energy landscape of the transesterification reaction between ethylbenzoate and methanol in implicit methanol solvent. The energies for reactant, transition, and product states were calculated through geometry optimizations. Energies for the reactant complex and product complex were obtained through geometry optimization of the final IRC structures in each respective direction.

Figure 6 shows that activation energy barriers for the transesterification reaction in implicit methanol solvent are very similar to those of in vacuum; thus, indicating that the implicit methanol solvent does not have any effect on the transesterification reaction energy barrier.

Unlike in the vacuum calculations, Figure 6 shows no correlation between the structure of tertiary amines and energy at the transition state. Furthermore, the energies at the transition state are indistinguishable for DMA, aromatic TMA, and TEA catalysts. There is no obvious reason why the addition of the implicit solvent model should reorder the relative ranking of catalytic effects observed in the reaction mechanism. These results with implicit solvation for the overall methanolysis reaction and a neutral catalyst thus suggest that the key step that defines the rate in the PET depolymerization during methanolysis must lie elsewhere. Based on this interpretation, we next explored the scenario in which the proton transfer step from methanol to ethyl benzoate in the PET depolymerization reaction involves the tertiary amine catalysts.

Catalysts Involvement in the Proton Transfer Step. In this section, we explore the scenario in which the tertiary amine catalysts are actively involved in the transesterification reaction of ethyl benzoate and methanol via proton transfer. Rather than having the transesterification as one single concerted step, we split the reaction into two successive parts: first, the proton transfer from the methanol to the ethyl benzoate, which then is followed by the breaking of the ester bond. Furthermore, in the first step, instead of having the proton transfer directly from the methanol oxygen to the ester of the ethyl benzoate, the proton would first transfer to the amine catalyst before being subsequently transferred to the ethyl benzoate. The two discrete steps of the proton transfer in the transesterification of ethyl benzoate in methanol are given below in Scheme 2.

Although the reaction mechanism presented in Schematic 2 seems similar to that presented in Figure 2a, where the scanning of the R1 bond independent of the R2 results in an unreasonable TS structure due to the very high TS energy of 120 kcal/mol, this reaction pathway merits another exploration as we now have tertiary amine catalysts that are actively involved in the transesterification reaction. The reaction energy for the proton transfer from methanol to the tertiary amine as defined by step 1 in Scheme 2 in both vacuum and implicit methanol is given in Table 2. Note that in the proton transfer energy calculations, we restrained either the N–H bond in the protonated catalyst, the C–O bond in methanol, or both the

Scheme 2. Proposed Steps for Proton Transfer During Transesterification of Ethyl Benzoate in Methanol

Table 2. Proton Transfer Energy as Defined by Step 1 in Schematic 2 That Were Calculated Using M06-2x/6-311++G(d,p), Experimental Yield of DMT Product from PET Depolymerization as Obtained from ref 30 and the Charge on N Atom in the Protonated Tertiary Amine Catalysts as Calculated by CHELPG Using the M06- $2x^{32}$ Functional and the 6-311++G(d,p)^{42,43} Basis Set

			ransfer energy cal/mol)		
catalysts	catalyst configuration	in vacuum	in implicit methanol	experiment yield of DMT (%) ³⁰	charge on N atom in protonated tertiary amine calculated in implicit methanol $ \\$
NMP	cyclic	27.7	14.9	100	0.19
linear TMA	linear	33.4	22.2		0.13
TEA	linear	32.8	21.8	91.2	0.16
TEEDA	diamine	29.9	22.5	80.1	-0.14
aromatic TMA	aromatic	33.3	25.7	25.8	-0.28
DMA	aromatic	26.7	21.1	6.4	-0.30

N-H and C-O bonds simultaneously during the geometry optimization step.

Unlike that in Figure 6 where the incorporation of the implicit methanol solvent does not affect the activation energy barriers, Table 2 clearly shows that the implicit solvent has substantially lowered the reaction energy for proton transfer. Lower energy indicates that proton transfer from methanol to catalyst is more favorable in implicit methanol than in vacuum. Lower energy also indicates the possibility of proton transfer to catalyst first to be a favorable first step for the overall reaction. This will be followed by proton transfer to ester oxygen to form the products. Hence, these results indicate that PET depolymerization in methanolysis could take place through multiple discrete steps instead of a single concerted step.

We compare our results to those of the experimental PET methanolysis.³⁰ In addition to calculating proton transfer energies, the charge on the protonated N atom of the tertiary amine catalyst was also determined. Both the experimental yield of DMT product obtained through PET depolymerization process in methanolysis using different tertiary amine catalysts and the calculated electronic charge on the N atom of the protonated tertiary amine catalysts in implicit methanol solvent of the catalyst are also given in Table 2.

First, we noticed that the proton energy transfer bears no correlation with the experimental DMT product yield that is reported in the literature.³⁰ Second, however, we found that the experimental DMT yield correlates with the charge on the N atom of the protonated tertiary amine. This correlation between the charge on the N atom of the tertiary amine and the experimental DMT yield is only seen for a protonated catalyst in implicit methanol. We then calculated the charge on the N atom of the catalyst for the neutral catalysts in both vacuum and implicit methanol and of the protonated catalysts in vacuum. In all of these cases, we have seen no correlation between the charge on the N atom of the catalyst to the experimental yield. Charges on N atom for all cases are reported in Supporting Information Table A4. Table 2 does not include values for experimental DMT yield of linear TMA as it is not part of the experimental study.

Discussion. Through our systematic investigation, we found that the charge on the N atom of the tertiary amine catalysts correlates directly with the product yield of the PET depolymerization product in experiments. Furthermore, we found that the correlation exists only for protonated catalysts in implicit methanol solvent. In general, our computational investigation into the PET depolymerization reaction in methanolysis in the presence of tertiary amine catalysts reveals

several important insights: (1) the PET depolymerization into DMT and EG in methanolysis (Scheme 1) consists of several discrete steps rather than one concerted step, (2) the tertiary amine catalyst is actively involved in the reaction, in which the proton transfer from methanol to ethyl benzoate occurs via the tertiary amine catalyst, and (3) the proton transfer from methanol to the tertiary amine catalyst is the first step of the reaction, Finally, (4) the charge on the N atom of the protonated tertiary amine directly corresponds to the experimental DMT product percentage yield.

The correlation between the charge on the N atom of the protonated tertiary amine and the experimental DMT yield can be explained by the Lewis basicity of the N atom in the tertiary amine. The more basic the N atom of the tertiary amine is, the more capable the tertiary amine molecule is in extracting protons from methanol. As a result, a higher DMT yield can be produced in the PET depolymerization in methanol solvent. In this study, the basicity of the tertiary amine is reflected in the changes in the charge on the N atom from -1 to the result presented in Table 2 for each catalyst.

Seeing the direct correlation between the charge on the N atom of the protonated tertiary amine and the experimental DMT yield, we then propose that we can use the charge on the N atom of the protonated tertiary amine catalysts as a descriptor to initially screen the tertiary amine catalysts. This allows one to gauge the efficiency of the tertiary amine in catalyzing the PET depolymerization reaction in methanolysis. It will aid in initial screening further since it involves only a quick calculation of the charge and eliminates the need for bench experiments.

We note that this direct correlation is specific to the tertiary amine catalysts listed in this study after investigating their role in catalyzing PET depolymerization in methanolysis. In the future, this conclusion could be further assessed by testing the accuracy of the descriptor, that is, the charge on the N atom. It would need to be tested against a wider range of tertiary amine catalysts, in which the experimental DMT yields are known. Furthermore, using the charge on the atoms of the protonated catalysts to gauge and screen its efficiency in catalyzing PET depolymerization in methanol can be extended to other types of catalysts, such as of those acetate-based or carbonate-based metal catalysts. ^{12,24–27}

CONCLUSIONS

In this study, we have done a systematic computational investigation into the PET depolymerization reaction in

methanol solvent. We found that the PET depolymerization reaction in methanol into DMT and EG consists of several discrete reaction steps rather than a single concerted step. Furthermore, in the presence of tertiary amine catalysts, we have found that the proton transfer from methanol to the tertiary amine catalyst is the first step in the PET depolymerization reaction in methanolysis. By comparing our results to that of the experimental yield, we found that the experimental yield directly correlates to the charge on the N atom of the protonated tertiary amine catalyst. We then propose that we can use the charge on the N atom of the protonated tertiary amine as a descriptor to quickly predict the suitability of other tertiary amine molecules as potential catalysts for PET depolymerization in methanolysis. To be able to find a descriptor that can be used to quickly screen the suitability of potential catalysts for PET depolymerization is of great interest as the efficiency of the potential catalysts can be quickly predicted without the need for experiments, which may result in the generation of environmentally harmful waste.

ASSOCIATED CONTENT

Supporting Information

The Supporting Information is available free of charge at https://pubs.acs.org/doi/10.1021/acs.jpca.4c02276.

Example input files for finding the transition state, IRC scan, geometry optimization calculations, relative energy of transition state for all catalyzed and uncatalyzed reactions with imaginary frequency values for verifying transition state, equations for showing how experimental yield is calculated, and nitrogen charge values in neutral and protonated catalysts (PDF)

AUTHOR INFORMATION

Corresponding Author

Jim Pfaendtner — Department of Chemical & Biomolecular Engineering, North Carolina State University, Raleigh, North Carolina 27695, United States; ⊙ orcid.org/0000-0001-6727-2957; Email: pfaendtner@ncsu.edu

Authors

Rishabh Sanghavi — Department of Chemical Engineering, University of Washington, Seattle, Washington 98195, United States

Nadia N. Intan — Department of Chemical Engineering, University of Washington, Seattle, Washington 98195, United States; Occid.org/0000-0003-1967-178X

Shaoqu Xie — Gene and Linda Voiland School of Chemical Engineering and Bioengineering, Washington State University, Pullman, Washington 99164, United States; School of Light Industry and Chemical Engineering, Guangdong University of Technology, Guangzhou 510006, P. R. China

Hongfei Lin — Gene and Linda Voiland School of Chemical Engineering and Bioengineering, Washington State University, Pullman, Washington 99164, United States; ⊚ orcid.org/ 0000-0001-8198-1493

Complete contact information is available at: https://pubs.acs.org/10.1021/acs.jpca.4c02276

Notes

The authors declare no competing financial interest.

ACKNOWLEDGMENTS

This work was supported by NSF award EFRI-2132219. The work was facilitated using computational, storage, and networking infrastructure provided by the Hyak supercomputer system, supported in part by the University of Washington and the UW Student Technology Fee Proposal program (award 2015-028).

REFERENCES

- (1) Geyer, R.; Jambeck, J. R.; Law, K. L. Production, Use, and Fate of All Plastics Ever Made. *Sci. Adv.* **2017**, 3 (7), No. e1700782-e1700782.
- (2) Li, T.; Vijeta, A.; Casadevall, C.; Gentleman, A. S.; Euser, T.; Reisner, E. Bridging Plastic Recycling and Organic Catalysis: Photocatalytic Deconstruction of Polystyrene via a C-H Oxidation Pathway. ACS Catal. 2022, 12 (14), 8155–8163.
- (3) Guo, B.; Vanga, S. R.; Lopez-Lorenzo, X.; Saenz-Mendez, P.; Ericsson, S. R.; Fang, Y.; Ye, X.; Schriever, K.; Bäckström, E.; Biundo, A.; et al. Conformational Selection in Biocatalytic Plastic Degradation by PETase. *ACS Catal.* **2022**, *12* (6), 3397–3409.
- (4) Jambeck, J. R.; Geyer, R.; Wilcox, C.; Siegler, T. R.; Perryman, M.; Andrady, A.; Narayan, R.; Law, K. L. Plastic Waste Inputs from Land into the Ocean. *Science* **2015**, 347 (6223), 768–771.
- (5) Hundertmark, T.; Mayer, M.; McNally, C.; Simons, T. J.; Witte, C. How Plastics Waste Recycling Could Transform the Chemical Industry, 2018. https://www.mckinsey.com/industries/chemicals/our-insights/how-plastics-waste-recycling-could-transform-the-chemical-industry (accessed Dec 12, 2018).
- (6) Cao, F.; Wang, L.; Zheng, R.; Guo, L.; Chen, Y.; Qian, X. Research and Progress of Chemical Depolymerization of Waste PET and High-Value Application of Its Depolymerization Products. *RSC Adv.* **2022**, *12* (49), 31564–31576.
- (7) Yang, W.; Liu, R.; Li, C.; Song, Y.; Hu, C. Hydrolysis of Waste Polyethylene Terephthalate Catalyzed by Easily Recyclable Terephthalic Acid. *Waste Manag* **2021**, *135*, 267–274.
- (8) Kang, M. J.; Yu, H. J.; Jegal, J.; Kim, H. S.; Cha, H. G. Depolymerization of PET into Terephthalic Acid in Neutral Media Catalyzed by the ZSM-5 Acidic Catalyst. *Chem. Eng. J.* **2020**, 398 (125655), 125655–125657.
- (9) Yoshioka, T.; Sato, T.; Okuwaki, A. Hydrolysis of waste PET by sulfuric acid at 150°C for a chemical recycling. *J. Appl. Polym. Sci.* **1994**, 52 (9), 1353–1355.
- (10) Wang, Y.; Zhang, Y.; Song, H.; Wang, Y.; Deng, T.; Hou, X. Zinc-Catalyzed Ester Bond Cleavage: Chemical Degradation of Polyethylene Terephthalate. *J. Clean. Prod.* **2019**, *208*, 1469–1475.
- (11) Song, X.; Hu, W.; Huang, W.; Wang, H.; Yan, S.; Yu, S.; Liu, F. Methanolysis of Polycarbonate into Valuable Product Bisphenol A Using Choline Chloride-Based Deep Eutectic Solvents as Highly Active Catalysts. *Chem. Eng. J.* **2020**, 388 (124324), 124324–124329.
- (12) Pham, D. D.; Cho, J. Low-Energy Catalytic Methanolysis of Poly(Ethyleneterephthalate). *Green Chem.* **2021**, 23 (1), 511–525.
- (13) Kurokawa, H.; Ohshima, M.; Sugiyama, K.; Miura, H. Methanolysis of Polyethylene Terephthalate (PET) in the Presence of Aluminium Tiisopropoxide Catalyst to Form Dimethyl Terephthalate and Ethylene Glycol. *Polym. Degrad. Stab.* **2003**, 79 (3), 529–533.
- (14) Pingale, N. D.; Palekar, V. S.; Shukla, S. R. Glycolysis of Postconsumer Polyethylene Terephthalate Waste. *J. Appl. Polym. Sci.* **2010**, *115* (1), 249–254.
- (15) Wang, H.; Liu, Y.; Li, Z.; Zhang, X.; Zhang, S.; Zhang, Y. Glycolysis of Poly(Ethylene Terephthalate) Catalyzed by Ionic Liquids. *Eur. Polym. J.* **2009**, 45 (5), 1535–1544.
- (16) Liu, B.; Lu, X.; Ju, Z.; Sun, P.; Xin, J.; Yao, X.; Zhou, Q.; Zhang, S. Ultrafast Homogeneous Glycolysis of Waste Polyethylene Terephthalate via a Dissolution-Degradation Strategy. *Ind. Eng. Chem. Res.* **2018**, 57 (48), 16239–16245.

- (17) Gupta, P.; Bhandari, S. Chemical Depolymerization of PET Bottles via Ammonolysis and Aminolysis. In *Recycling of Polyethylene Terephthalate Bottles*; Elsevier, 2019; pp 109–134.
- (18) Crippa, M.; Morico, B. PET Depolymerization: A Novel Process for Plastic Waste Chemical Recycling. *Stud. Surf. Sci. Catal.* **2020**, *179*, 215–229.
- (19) Carniel, A.; Waldow, V. d. A.; Castro, A. M. de. A Comprehensive and Critical Review on Key Elements to Implement Enzymatic PET Depolymerization for Recycling Purposes. *Biotechnol. Adv.* **2021**, *52* (107811), 107811–107815.
- (20) Lee, H. L.; Chiu, C. W.; Lee, T. Engineering Terephthalic Acid Product from Recycling of PET Bottles Waste for Downstream Operations. *Chem. Eng. J. Adv.* **2021**, *5* (100079), 100079–100114.
- (21) da Costa, A. M.; de Oliveira Lopes, V. R.; Vidal, L.; Nicaud, J.-M.; de Castro, A. M.; Coelho, M. A. Z. Poly(Ethylene Terephthalate) (PET) Degradation by Yarrowia Lipolytica: Investigations on Cell Growth, Enzyme Production and Monomers Consumption. *Process Biochem.* **2020**, *95*, 81–90.
- (22) Duh, B. Reaction Kinetics for Solid-State Polymerization of Poly(Ethylene Terephthalate). *J. Appl. Polym. Sci.* **2001**, *81* (7), 1748–1761.
- (23) Lawal, M. M.; Govender, T.; Maguire, G. E. M.; Kruger, H. G.; Honarparvar, B. DFT Study of the Acid-Catalyzed Esterification Reaction Mechanism of Methanol with Carboxylic Acid and Its Halide Derivatives. *Int. J. Quantum Chem.* **2018**, *118* (4), No. e25497-e25497
- (24) Baliga, S.; Wong, W. T. Depolymerization of Poly(Ethylene Terephthalate) Recycled from Post-Consumer Soft-Drink Bottles. *J. Polym. Sci. Part A Polym. Chem.* **1989**, 27 (6), 2071–2082.
- (25) Xi, G.; Lu, M.; Sun, C. Study on Depolymerization of Waste Polyethylene Terephthalate into Monomer of Bis(2-Hydroxyethyl Terephthalate). *Polym. Degrad. Stab.* **2005**, 87 (1), 117–120.
- (26) Ghaemy, M.; Mossaddegh, K. Depolymerisation of Poly-(Ethylene Terephthalate) Fibre Wastes Using Ethylene Glycol. *Polym. Degrad. Stab.* **2005**, *90* (3), 570–576.
- (27) Shukla, S. R.; Kulkarni, K. S. Depolymerization of Poly-(Ethylene Terephthalate) Waste. *J. Appl. Polym. Sci.* **2002**, 85 (8), 1765–1770.
- (28) Bao, Y.-S.; Zhaorigetu, B.; Agula, B.; Baiyin, M.; Jia, M. Aminolysis of Aryl Ester Using Tertiary Amine as Amino Donor via C-O and C-N Bond Activations. *J. Org. Chem.* **2014**, 79 (2), 803–808
- (29) Oliveri, I.; Di Bella, S.; Di Bella, S. Sensitive Fluorescent Detection and Lewis Basicity of Aliphatic Amines. *J. Phys. Chem. A* **2011**, *115* (50), 14325–14330.
- (30) Lin, H. Conversion of Co-Mingled Waste Plastics to Monomers and Fuels in Sequential Catalytic Process. No. 18/251,958, filed November 9, 2021. https://ppubs.uspto.gov/dirsearch-public/print/downloadPdf/20240025085 (accessed Nov 9, 2021).
- (31) Frisch, M. J.; Trucks, G. W.; Schlegel, H. B.; Scuseria, G. E.; Robb, M. A.; Cheeseman, J. R.; Scalmani, G.; Barone, V.; Petersson, G. A.; Nakatsuji, H.; et al. *Gaussian 16*. Revision C.01; Gaussian, Inc.: Wallingford, CT, 2016.
- (32) Zhao, Y.; Truhlar, D. G. The M06 suite of density functionals for main group thermochemistry, thermochemical kinetics, non-covalent interactions, excited states, and transition elements: two new functionals and systematic testing of four M06-class functionals and 12 other functionals. *Theor. Chem. Acc.* 2008, 120 (1–3), 215–241.
- (33) Francl, M. M.; Pietro, W. J.; Hehre, W. J.; Binkley, J. S.; Gordon, M. S.; DeFrees, D. J.; Pople, J. A. Self-Consistent Molecular Orbital Methods. XXIII.A Polarization-Type Basis Set for Second-Row Elements. *J. Chem. Phys.* **1982**, *77* (7), 3654–3665.
- (34) Hehre, W. J.; Ditchfield, R.; Pople, J. A. Self—Consistent Molecular Orbital Methods. XII. Further Extensions of Gaussian—Type Basis Sets for Use in Molecular Orbital Studies of Organic Molecules. *J. Chem. Phys.* **1972**, *56* (5), 2257–2261.
- (35) Cammi, R.; Tomasi, J. Remarks on the Use of the Apparent Surface Charges (ASC) Methods in Solvation Problems: Iterative

- versus Matrix-Inversion Procedures and the Renormalization of the Apparent Charges. J. Comput. Chem. 1995, 16 (12), 1449–1458.
- (36) Miertuš, S.; Scrocco, E.; Tomasi, J. Electrostatic Interaction of a Solute with a Continuum. A Direct Utilizaion of AB Initio Molecular Potentials for the Prevision of Solvent Effects. *Chem. Phys.* **1981**, *55* (1), 117–129.
- (37) Mennucci, B.; Cancès, E.; Tomasi, J. Evaluation of Solvent Effects in Isotropic and Anisotropic Dielectrics and in Ionic Solutions with a Unified Integral Equation Method: Theoretical Bases, Computational Implementation, and Numerical Applications. *J. Phys. Chem. B* 1997, 101 (49), 10506–10517.
- (38) Cancès, E.; Mennucci, B.; Tomasi, J. A New Integral Equation Formalism for the Polarizable Continuum Model: Theoretical Background and Applications to Isotropic and Anisotropic Dielectrics. *J. Chem. Phys.* **1997**, *107* (8), 3032–3041.
- (39) Cancès, E.; Mennucci, B. New Applications of Integral Equations Methods for Solvation Continuum Models: Ionic Solutions and Liquid Crystals. *J. Math. Chem.* **1998**, *23*, 309–326.
- (40) Li, X.; Frisch, M. J. Energy-Represented Direct Inversion in the Iterative Subspace within a Hybrid Geometry Optimization Method. *J. Chem. Theory Comput.* **2006**, 2 (3), 835–839.
- (41) Fukui, K. The Path of Chemical Reactions the IRC Approach. Acc. Chem. Res. 1981, 14 (12), 363–368.
- (42) Breneman, C. M.; Wiberg, K. B. Determining Atom-Centered Monopoles from Molecular Electrostatic Potentials. The Need for High Sampling Density in Formamide Conformational Analysis. *J. Comput. Chem.* **1990**, *11* (3), 361–373.
- (43) Krishnan, R.; Binkley, J. S.; Seeger, R.; Pople, J. A. Self-Consistent Molecular Orbital Methods. XX.A Basis Set for Correlated Wave Functions. *J. Chem. Phys.* **1980**, 72 (1), 650–654.
- (44) Clark, T.; Chandrasekhar, J.; Spitznagel, G. W.; Schleyer, P. V. R. Efficient Diffuse Function-Augmented Basis Sets for Anion Calculations. III. The 3-21+G Basis Set for First-Row Elements, Li-F. J. Comput. Chem. 1983, 4 (3), 294–301.
- (45) The PLUMED consortium. Promoting transparency and reproducibility in enhanced molecular simulations. *Nat. Methods* **2019**, *16* (8), 670–673.
- (46) Tribello, G. A.; Bonomi, M.; Branduardi, D.; Camilloni, C.; Bussi, G. PLUMED 2: New Feathers for an Old Bird. *Comput. Phys. Commun.* **2014**, *185* (2), 604–613.
- (47) Kenouche, S.; Belkadi, A.; Djebaili, R.; Melkemi, N. High Regioselectivity in the Amination Reaction of Isoquinolinequinone Derivatives Using Conceptual DFT and NCI Analysis. *J. Mol. Graph. Model.* **2021**, *104*, 107828.
- (48) Sarala, S.; Geetha, S. K.; Muthu, S.; Irfan, A. Probing Solvent Effect and Strong and Weak Interactions in 2-Nitrophenyl-Hydrazine Using Independent Gradient Model and Hirshfeld from Wave Function Calculation. *J. Mol. Liq.* **2021**, *341*, 117345.
- (49) Borges, I. D.; Danielli, J. A. V.; Silva, V. E. G.; Sallum, L. O.; Queiroz, J. E.; Dias, L. D.; Iermak, I.; Aquino, G. L. B.; Camargo, A. J.; Valverde, C.; et al. Synthesis and Structural Studies on (E)-3-(2,6-Difluorophenyl)-1-(4-Fluorophenyl)Prop-2-En-1-One: A Promising Nonlinear Optical Material. *RSC Adv.* **2020**, *10* (38), 22542–22555.
- (50) Silva, P. L.; Silva, C. M.; Guimarães, L.; Pliego, J. R. Acid-Catalyzed Transesterification and Esterification in Methanol: A Theoretical Cluster-Continuum Investigation of the Mechanisms and Free Energy Barriers. *Theor. Chem. Acc.* **2015**, *134* (1), 1591.